e-Prime - Advances in Electrical Engineering, Electronics and Energy 12 (2025) 101033

Contents lists available at ScienceDirect

e-Prime - Advances in Electrical Engineering, Electronics and Energy

journal homepage: www.elsevier.com/locate/prime

Junction temperature prediction Model Development with Co-simulation

Mustafa Ozden [a,b,*], Gokhan Ozkan [a,b], S M Imrat Rahman [a], Elutunji Buraimoh [a], Laxman Timilsina [a], Behnaz Papari [a,c], Christopher S. Edrington [a]

[a] Holcombe Department of Electrical and Computer Engineering, Clemson, 29634, SC, USA
[b] Dominion Energy Innovation Center, North Charleston, 29405, SC, USA
[c] Department of Automotive Engineering, Greenville, 29607, SC, USA

ARTICLE INFO

Keywords:
Junction temperature prediction
Temperature-responsive power loss calculation (TRPLC)
Temperature-agnostic power loss calculation (TAPLC)
Neutral Point Clamped Converter (NPC)

ABSTRACT

This study examines the thermal behavior and junction temperature of MOSFET modules under varying operating conditions using ANSYS/Fluent software, with simulations managed through Python/Jupyter Notebook. Two different approaches are evaluated: the Temperature-Responsive Power Loss Calculation (TRPLC) and the Temperature-Agnostic Power Loss Calculation (TAPLC). In the TRPLC approach, power loss is calculated as a func- tion of the junction temperature, which is updated at each time step. In contrast, the TAPLC approach relies on four predefined power loss curves derived from the MOSFET datasheet, with each curve simulated separately. Unlike TRPLC, this method does not account for the relationship between junction temperature and power loss, resulting in significantly high junction temperature values at higher power loss levels. By dynamically recalculating power loss at every step, the TRPLC approach provides more realistic results compared to TAPLC. These findings underscore the importance of incorporating temperature-dependent calculations to enhance the accuracy of thermal performance predictions under practical operational scenarios.

1. Introduction

Semiconductor devices are foundational elements in modern energy sys- tems, playing critical roles in the integration of renewable energy sources, battery storage, and electric vehicle technologies [1,2]. Looking ahead, the integration of semiconductor devices into smart grid technologies and electric vehicles will continue to drive innovation in energy systems. Likewise, the increasing integration of renewable energy sources, such as solar and wind power, demands advanced power electronics systems for efficient energy con- version and management.

The reliable operation of semiconductor devices is essential for the sta- bility of the electrical grid and the efficiency of energy conversion processes. Power electronics systems long-term performance and dependability depend heavily on effective thermal management [3]. Semiconductor devices with ad- vanced control algorithms, real-time monitoring, and predictive maintenance contribute significantly to enhancing system performance and ensuring con- sistent operation [4]. Moreover, the development of advanced cooling strate- gies and enhanced thermal management systems will be critical in meeting the increasing demands of future energy systems [4]. Given its importance, thermal management is also essential for addressing thermal stress, which occurs when temperature changes affect the performance of power electronic components, particularly power semiconductors. Managing thermal stress on critical components remains a significant challenge in power electronics, highlighting the necessity for robust and efficient cooling solutions [5]. Var- ious techniques, including passive and active cooling methods, have been developed to address the challenge of managing the thermal stress [6]. Pas- sive cooling methods, such as heat sinks and thermal interface materials, rely on natural convection to dissipate heat [7]. Active cooling methods [8], such as fans and liquid cooling systems [7–9] provide more efficient heat dissipation but require additional components and energy consumption [10]. To manage thermal stress and develop effective thermal management al- gorithms, understanding the thermal behavior of semiconductor and power electronic systems is essential. MOSFET chips are the components that heat up the most compared to other components in the power electronic system because they allow a high amount of energy to be transferred through the material. Although it is not easy to measure or estimate the temperature from these devices, it is possible with the experimental and numerical methods developed [11]. Experimental methods offer high reliability but are often challenging to implement and expensive. On the other hand, numerical ap- proaches, such as finite

* Corresponding author.
E-mail address: mozden@clemson.edu (M. Ozden).

https://doi.org/10.1016/j.prime.2025.101033
Received 18 February 2025; Received in revised form 2 May 2025; Accepted 25 May 2025
Available online 29 May 2025

element analysis (FEA), are widely used to predict temperature using computer-aided software [12,13]. Although numerical methods offer many advantages, they require careful preparation and implementation. FEA, in particular, provides accurate results by integrating experimental data into energy equations.

Progress in computational fluid dynamics (CFD) software, enhanced com- puting power, and co-simulation-based software integration has driven the creation of advanced thermal models. Additionally, with the development of real-time simulators, data obtained from experimental systems can also be incorporated into simulations. This study focuses on improving junction temperature prediction by analyzing one leg of a three-phase power converter using two different softwares.

1.1. Contribution of the paper

This study clarifies the development of approaches in CFD analysis methods used for junction temperature estimation. It introduces new methods to improve the accuracy of junction temperature predictions. The key contri- butions of this paper include:

- Introduction of the Temperature-Responsive Power Loss Calculation: The paper presents a novel approach where power loss is recalculated at each time step based on the junction temperature, rather than rely- ing on fixed power losses. This method accounts for dynamic changes in temperature and provides a more accurate estimation of junction temperatures.
- Integration of 3D Thermal Analysis: The study integrates 3D thermal analysis into the CFD models, considering real-world parameters such as cold plate design, coolant flow rate, coolant temperature, and ambi- *ent* conditions. This allows for a more realistic simulation environment, closely mirroring actual operating conditions.
- Evaluation of Traditional vs. Modern Approaches: The research provides a comparative analysis between traditional fixed-temperature power loss calculations and the proposed temperature-responsive approach. This comparison highlights the limitations of existing methods and un- derscores the benefits of adopting time-sensitive calculations.
- Recommendations for Future Simulations: The paper offers practical recommendations for researchers and engineers to implement transient thermal simulations in their designs, emphasizing the importance of accounting for transient thermal behaviors in power electronic devices.

The paper is structured as follows. Section 2 discusses the methodology and modeling of the proposed framework. Section 3 presents validation of the CFD model and Co-simulation results. Section 4 concludes the paper.

2. Methodology and modeling

2.1. Working process of SIC MOSFET devices in a three-level NPC model

Voltage-source multilevel converters are widely utilized in modern power electronics and are categorized based on their circuit configurations and the method of generating output voltage levels. This classification is determined by the structural arrangement of components, such as capacitors, clamping diodes, and H-bridge modules, which directly influence the operational char- acteristics and application range of the converters [11]. Based on these topo- logical distinctions, voltage-source multilevel converters are generally divided into three main categories: flying capacitor (FLC), neutral point clamped (NPC), and cascade H-bridge [14].

Among these, the Neutral-Point-Clamped (NPC) converter stands out for its extensive use in medium and high-voltage applications, where its three- level topology provides significant advantages over traditional two-level de- signs [15]. By splitting the total voltage across multiple devices, NPC converters reduce the voltage stress on individual semiconductors, enhancing their reliability and lifespan. Compared to two-level converters, where the entire DC bus voltage is switched across the power devices, the NPC con- verter's three-level design allows for smaller voltage steps, resulting in more efficient operation. Additionally, the increased number of voltage vectors in NPC converters enables finer control of the output waveform, reducing harmonic distortion and mitigating stress on motor windings in motor drive applications [16].

To control the fundamental voltage functions of a three-level NPC con- verter, three primary techniques have been developed: carrier-based PWM, space vector modulation (SVM), and selective harmonic elimination (SHE). Each method offers unique benefits in balancing performance and harmonic mitigation, making NPC converters a preferred choice for advanced indus- trial and renewable energy systems. These advantages underscore the role of NPC converters as a cornerstone of modern power electronics, combining efficiency, reliability, and precise control to meet the demands of complex applications.

Despite the numerous advantages of Neutral-Point-Clamped (NPC) con- verters, such as efficient control mechanisms and reduced power losses, they are not exempt from the common challenge faced by all electronic systems: heat generation. Proper thermal management is essential to ensure the re- liability and performance of these systems. While various cooling solutions are available, this study employs a liquid-based cooling system to address the thermal challenges.

The primary components of the liquid cooling system, namely the chiller and the cold plate, are illustrated in Fig. 1. Additionally, the NPC con- verter design is depicted in the same figure, highlighting the arrangement of key components. Each leg of the converter contains two MOSFET modules and one diode module, all of which are clearly indicated. This integration of cooling components and converter design ensures effective heat dissipation, thereby enhancing the overall operational stability of the system.

The SiC 3 Level NPC converter can operate at a higher switching frequency thanks to the SiC MOSFET's reduction of switching energies. Hence, the SiC 3 Level NPC converter's AC output filter size is decreased. To pro- vide a clearer explanation of the switch states (1,0,−1),the possible positions on the two H-bridge MOSFET modules in the design are illustrated in Fig. 2.

Fig. 2 illustrates the top view of a single leg of the Neutral-Point-Clamped (NPC) converter, showcasing the structural arrangement and oper- ational states of its components. The leg comprises two MOSFET modules and one diode module. Each MOSFET module functions as an H-bridge, incorporating two MOSFETs designated as the "upper switch" (top MOSFET) and the "lower switch" (bottom MOSFET). The figure also demon- strates three distinct switching states of the NPC converter leg, which are integral to the Space Vector Modulation (SVM) technique.

- State 0 (O): In this state, the lower switch of the first MOSFET module and the upper switch of the second MOSFET module are active. This configuration results in a neutral output voltage, ensuring balanced operation and minimal power flow.
- State +1 (P): Here, both the upper and lower switches of the first MOSFET module are engaged. This state corresponds to a positive output voltage vector and directs current flow to achieve specific voltage waveforms required for load control.
- State −1 (N): In the final state, the upper and lower switches of the second MOSFET module are activated. This state generates a negative output voltage vector, completing the three primary switching positions for the converter leg.

These three states labeled as +1 (P), 0 (O), and −1 (N)—are part of the fundamental switching combinations used in Space Vector Modulation (SVM). By systematically transitioning between these states, SVM achieves precise control over the converter's output waveform, improving harmonic performance and minimizing losses.

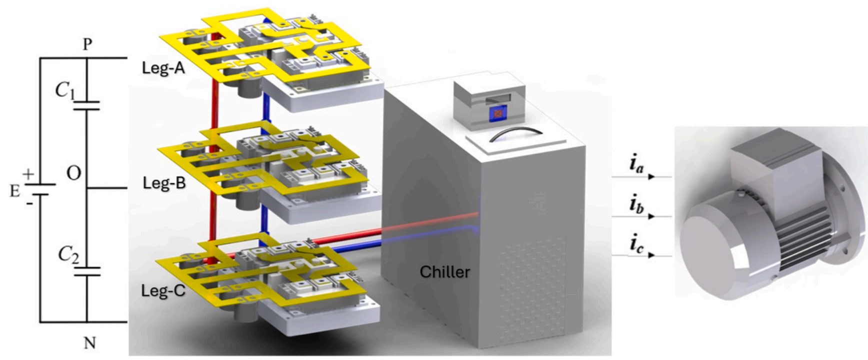

Fig. 1. 3D Design model of the converter with cooling system.

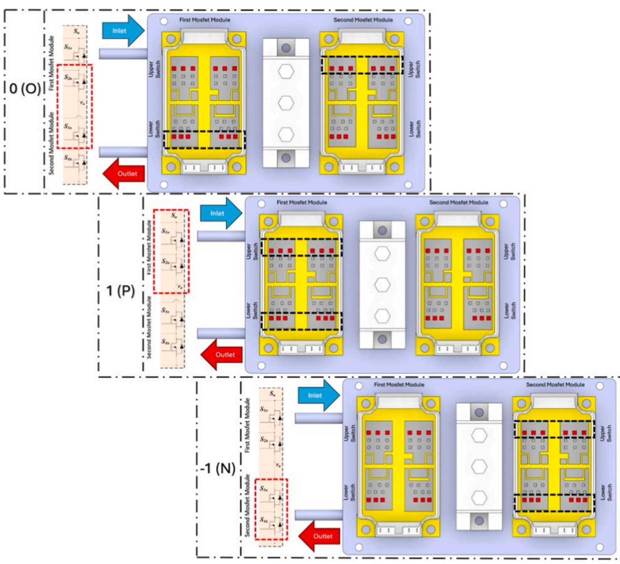

Fig. 2. Top view of the case and the possible switch states.

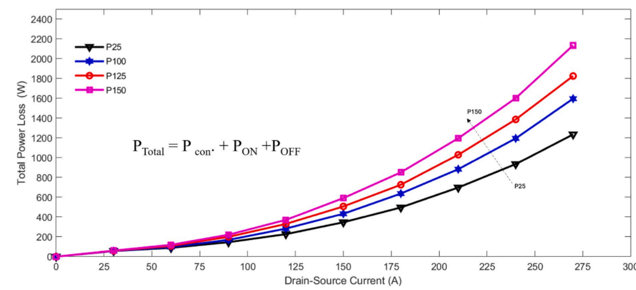

Fig. 3. Power loss characteristic with drain-source current.

Fig. 2 also shows the locations of the cold plate inlet and outlet surfaces. The MOSFET closer to the inlet can be cooled more than the others, which is an expected result.

2.2. Semiconductor device power loss calculation

Power losses in power electronic switching devices can generally be cate- gorized into two types: dynamic loss and static loss. Dynamic losses include turn-on and turn-off losses, while static losses comprise con- duction loss (on- state power loss) and cut-off loss. MOSFET manufac- turers typically provide power loss graphs in their datasheets, which illustrate the relationship be- tween power loss, drain-source current, and junction temperature [17]. While these graphs are useful for un- derstanding the thermal and electrical behavior of a single MOSFET module, they do not provide sufficient information for predicting the performance of multiple MOSFET modules operating together in com- plex systems.

To address this limitation and adapt the available data for CFD mod- els, the power loss components conduction loss, turn-on loss, and turn- off loss were combined into a single power loss value. Using the data provided in the datasheets, power loss curves were generated as func- tions of junc- tion temperature and drain-source current. Four specific curves, named P25, P100, P125, and P150, corresponding to different junction temperature values, were created. Intermediate power loss values were calculated through interpolation techniques using the equations derived from these curves (Fig. 3).

This approach ensures that the power loss behavior of MOSFET modules is accurately represented in the CFD model, capturing the de- pendencies on both junction temperature and drain-source current. These interpolated power loss curves provide a comprehensive basis for analyzing and optimizing the thermal and electrical performance of multiple MOSFET modules in power electronic systems.

2.3. CFD modeling and thermal characteristic

Establishing an accurate thermal model is critical to the electro- thermal design of power electronic devices. This study presents a computational fluid dynamics (CFD) model designed to determine the junction temperature of MOSFETs. CFD analysis is a numerical simula- tion method that employs fundamental equations of fluid dynamics and heat transfer, along with ma- terial properties, to calculate various physical phenomena, including heat dissipation. The junction temper- ature depends not only on power dissipa- tion but also on external fac- tors such as variations in coolant flow rate or ambient temperature fluctuations caused by other devices in the same cooling system.

The system components were discussed in the previous section of the paper. In this section, the design and analysis methods used in the CFD model will be elaborated. CFD software recommends refining and making assumptions about geometric details to facilitate the creation of network structures and reduce analysis time. During geometry forma- tion, it was considered that two different fluids were present: the cooling fluid (water) circulating in the cold plate and the air in the environment. Meshing is another crucial aspect of simulation and should be approached with care. In the mesh structure created with the ANSYS Mechanical module, a dense mesh is applied to small geometries such as SiC chips, while a coarser mesh is used in the flow region compared to the mesh on the SiC chip.

In Fig. 4, a schematic representation has been added to demonstrate the transformation of one leg of a three-leg converter into its CAD design. The visualization focuses on one leg of the converter, high- lighting the placement of two MOSFET modules and their switches within the overall con- verter.

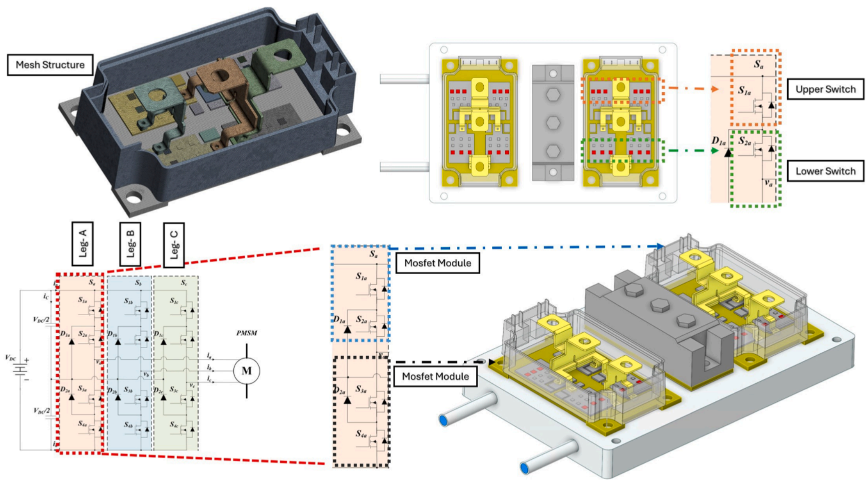

Fig. 4. CFD Mesh of the one-leg converter.

The definition of boundary conditions and thermal simulation parameters for the CFD model is performed in the Fluent module. The ambient fluid is set to air at a temperature of 49 °C. The cooling fluid circulating in the cold plate is defined as water, with a temperature and flow rate of 49 °C and 1 LPM, respectively.

CFD's basic concept is to divide the entire computational domain into separate small-scale parts and calculate local solutions to the diffusion con- vection reaction problem [18].

The behavior of fluid substances within the computational fluid dynam- ics (CFD) model is governed by the Navier-Stokes equations, which describe the conservation of momentum, mass, and energy. These equations con- sist of several components, including velocity (m/s), pressure (Pa), density (kg/m^3), and viscosity ($Pa \cdot s$). The general forms of the governing equations are as follows:

Continuity Equation:

$$\frac{\partial \rho}{\partial t} + \nabla(\rho\mu) = 0 \tag{1}$$

Momentum Equation:

$$\frac{\partial}{\partial t}(\rho\mu) + \nabla(\rho\mu\mu) = -\nabla\rho + \nabla(\mu\nabla\mu) + \rho g + \mathrm{F} \tag{2}$$

Here, ρ is the density of the fluid (kg/m^3), $\mathbf{u}$ represents the velocity vector (m/s), t is time (s), p is pressure (Pa), μ is the dynamic viscosity ($Pa \cdot s$), and $\mathbf{F}$ encompasses body forces, such as gravity (N/kg).

The conservation of energy is modeled using the energy equation, which considers the transport of thermal, kinetic, and potential energy.

Energy Equation:

$$\frac{\partial}{\partial t}(\rho E) + \nabla\cdot(\mathrm{u}(\rho E + p)) = \nabla\cdot(k\nabla T) + \Phi \tag{3}$$

In this equation, T is the temperature (K), k is the thermal conductivity (W/mK), S represents the source term (including internal heat generation, W/m^3), and Φ denotes viscous heat generation.

2.4. Python / pyfluent library

There are various methods for the automated control of ANSYS Fluent software, such as user-defined functions (UDF), profile definitions, and the MATLAB-ANSYS interface. If these methods are considered in order, using UDF to manipulate and run a simulation in Fluent requires uploading a C file into the user-defined function section of Fluent. It is a useful method for progressing a parameter within the simulation in a time-dependent or iterative manner, but it is not possible to provide feedback from simulation outputs to inputs using UDF. Similarly, UDFs can be manipulated within MATLAB and executed with Fluent, but the issue with this method is that every time MATLAB runs the UDF, Fluent is restarted, which prevents continuity in the simulation. The MATLAB-ANSYS interface is a set of MATLAB codes supported by older versions. In recent versions, this interface is no longer supported. Due to the growing popularity of Python, especially in the field of machine learning, and its ease of use, researchers developed the PyFluent library. With PyFluent, many processes from geometry setup to analysis and the evaluation of results can be managed efficiently. The main contribution of PyFluent to this study is the ability to automate Fluent simulations and dynamically evaluate results, allowing for new parameters to be defined based on conditions.

2.5. Python and ansys fluent co-simulation framework

The growing importance of energy conservation in power electronics has led researchers to rely on simulation software during the design phase and optimization to minimize the impact of the switching mechanism and reduce implementation costs [19–21]. Numerical simulation methods that encompass multiple physics fields are widely utilized in the research of MOSFET module package optimization, junction temperature monitoring, aging evaluation, and failure analysis [22,23].

The proposed co-simulation of Python and ANSYS/Fluent can be divided into two parts: running Fluent software via Python/Jupyter Notebook (JN) (TAPLC), power loss calculation depending on the junction temperature with JN, and running the simulation (TRPLC). JN provides power loss, switch state, and cooler flow rate to Fluent. Fluent provides junction temperature to JN.

The customized thermal model is loaded into Fluent, which is launched via Python/JN. Once both programs are ready for co-simulation, JN sends the power loss, cooler velocity, cooler temperature, and switch states as inputs to Fluent. After Fluent completes the simulation, the output parameters are read by Python, which calculates the new power loss value. This updated value, along with the other parameters, is sent back to Fluent as input for the next simulation step (Fig. 5). The simulation continues in a loop until all the data in the drain-source current profile are processed. Here is how the TRPLC operates.

In TRPLC, all equations related to the curves shown in Fig. 3 are used within the simulation. However, in TAPLC, since the junction temperature is not read at each step, a separate simulation is conducted for each equation.

3. Simulation results

In this section, the results obtained from CFD model and co-simulation are examined. First, the thermal conductivity of the DBC

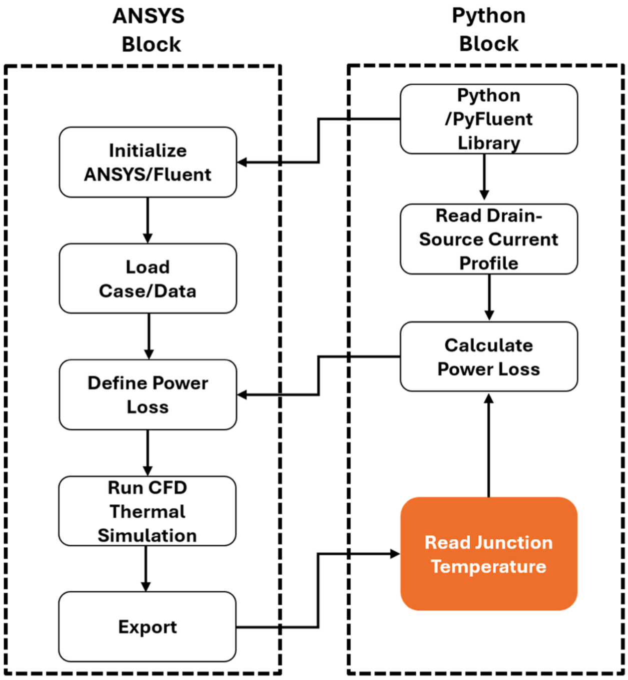

Fig. 5. Flow chart of the electro-thermal co-simulation (TRPLC).

layer in the MOSFET module, which initially had unknown thermal properties, was deter- mined, and model validation was performed. Following the validation study, co-simulation results for various scenarios were analyzed and discussed in detail.

3.1. Model validation with case temperature

MOSFET modules (CAS120M12BM2) are highly specialized structures with an architecture comprising complex layered designs and small compo- nents. Manufacturers provide case temperatures in relation to power dissi- pation in their data sheets. If the case temperature is known, the junction temperature can be estimated to determine whether it remains within the device's safe operating limits. Using case temperature and power dissipation information, it is possible to infer the thermal conductivities of materials in the layers of the 3D geometries created for analysis. The thermal properties of the SiC and copper layers were taken from the studies of Shuai et al. [11], while the thermal properties of the DBC layer were analyzed independently [24]. In this study, the bottom surface of the MOSFET module, named the baseplate, was fixed at the case temperatures shown in Fig. 6. Power losses were then defined separately according to the values presented in the visual. The thermal conductivity of the DBC layer was adjusted to ensure that the junction temperature remained below 150 °C. The thermal

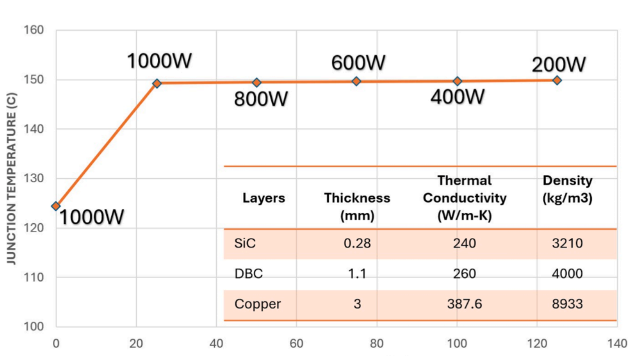

Fig. 6. Junction temperature depending on case temperature.

conductivities for the SiC, DBC, and copper layers were determined to be 240 W/mK, 260 W/mK, and 387.6 W/mK, respectively.

3.2. Co-Simulation results

The results of the co-simulation analysis, conducted by integrating Jupyter Notebook with Fluent software through Python scripting, are presented in this section. The co-simulation allowed for a detailed examination of the thermal behavior of the MOSFET module.

The differences in junction temperature resulting from the variations in approach between the Temperature-Responsive Power Loss Calculation (TRPLC) and the Temperature-Agnostic Power Loss Calculation (TAPLC) methods, as detailed in Section 2, are illustrated in Fig. 7. The two MOSFET switches within each of the two MOSFET modules used in the system are evaluated separately, with their positions depicted in Fig. 2 in Section 2. As MOSFET structures are designed in a half-bridge configuration, each module includes two MOSFET switches. Figs. 7(a) and 7 (b) present the results for the upper and lower switches of the first MOSFET module, respectively. Similarly, Figs. 7(c) and 7 (d) display the results for the upper and lower switches of the second MOSFET module.

In Figs. 7(a) and 7 (b), the maximum junction temperatures predicted by TRPLC are 95.1 °C and 96.4 °C for the upper and lower switches of the first MOSFET module, respectively. The closest results to these tempera- tures are provided by the P100, with values of 97.2 °C and 98.5 °C, respectively. Similar to the first MOSFET module, the second MOSFET module results are 113.2 °C (Fig.7(c)) and 114.8 °C (Fig. 7(d). Likewise, the closest comparison is observed in the P100 solution, with values of 110.5 °C and 112.3 °C, respectively. While the results of TRPLC and P100 are fairly similar, significant differences are observed when compared to the results of P125, P150, and P25.

As shown in Fig. 7, the junction temperatures observed in solutions em- ploying P150 and P125 are significantly higher compared to other equations and TRPLC. Conversely, the results for P25 demonstrate much lower temperatures relative to the others. The results obtained from solutions using P100 are generally close to those of TRPLC. In Fig. 7, the maximum junc- tion temperatures are illustrated in detail views. Upon detailed examination of these views, it is observed that the results from P100 exhibit lower tem- peratures than TRPLC on both switches of the first MOSFET module. On the other hand, the junction temperatures obtained on the switches of the second MOSFET module show that TRPLC results are higher than those of P100.

The differences in temperatures predicted by TRPLC compared to those obtained from P100 on the switches of the first MOSFET module are at- tributed to the dynamic calculation strategy employed by TRPLC. Similarly, higher junction temperature values in the second MOSFET module for TR- PLC results further demonstrate its ability to adapt to real-time thermal behavior.

The results underscore the critical importance of selecting the correct equation based on junction temperature. In the upper switch of the first MOSFET module, the maximum temperature difference between P150 and P25 is 29.1 °C, while in the lower switch, the difference is 29.8 °C. In the upper switch of the second MOSFET module, a maximum temperature difference of 37.1 °C is observed, while the lower switch shows a difference of 38.3 °C. These temperature differences highlight the necessity of using TRPLC approaches in thermal simulations for MOSFET modules.

Heat maps and contour visuals are highly effective tools for observing and understanding temperature variations [25]. Figs. 8(a) and 8 (b) show the TRPLC and TAPLC P150 results for $t = 4.31$ s and 4.43 s, respectively. To facilitate comparison, the same legend has been used. These visuals not only demonstrate how the temperature is distributed from the chips across the entire system but also show the continuity of the heat effect that was generated in the previous position after the switch state change.

In Fig. 8, at $t = 4.31$ s, both switches of the second MOSFET mod-ule are high, leading to higher temperature compared to the first MOSFET

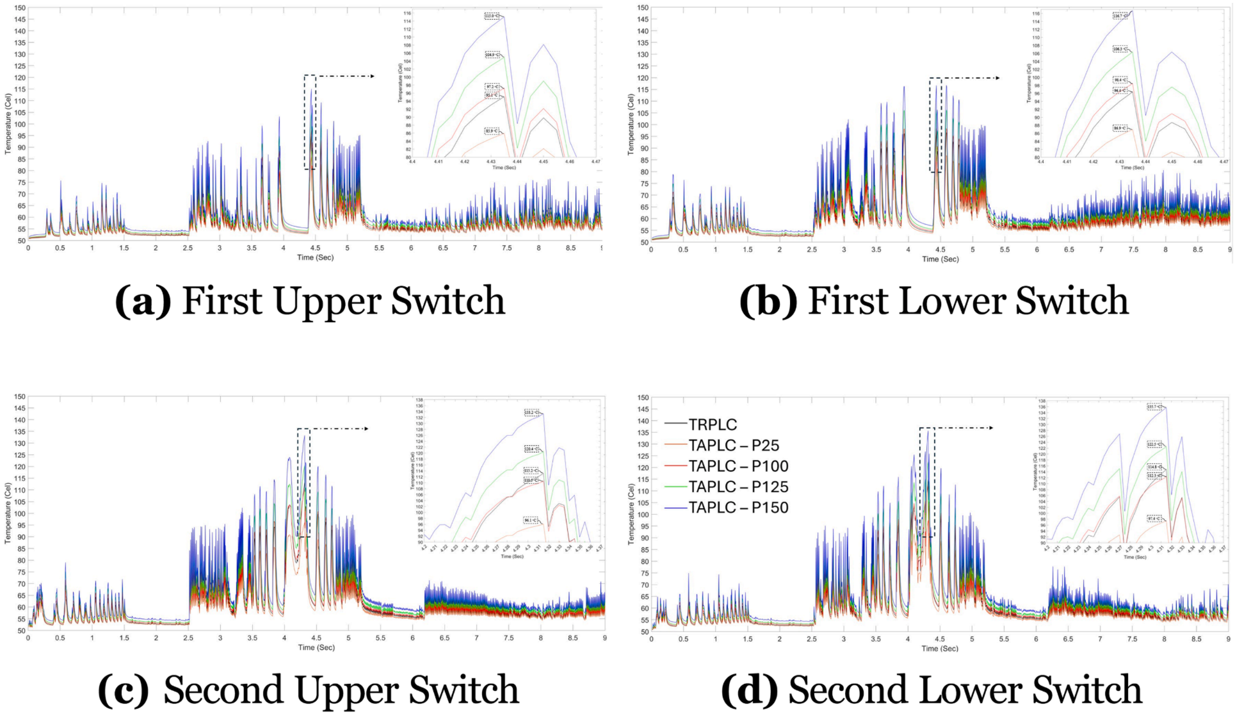

Fig. 7. Junction temperature results.

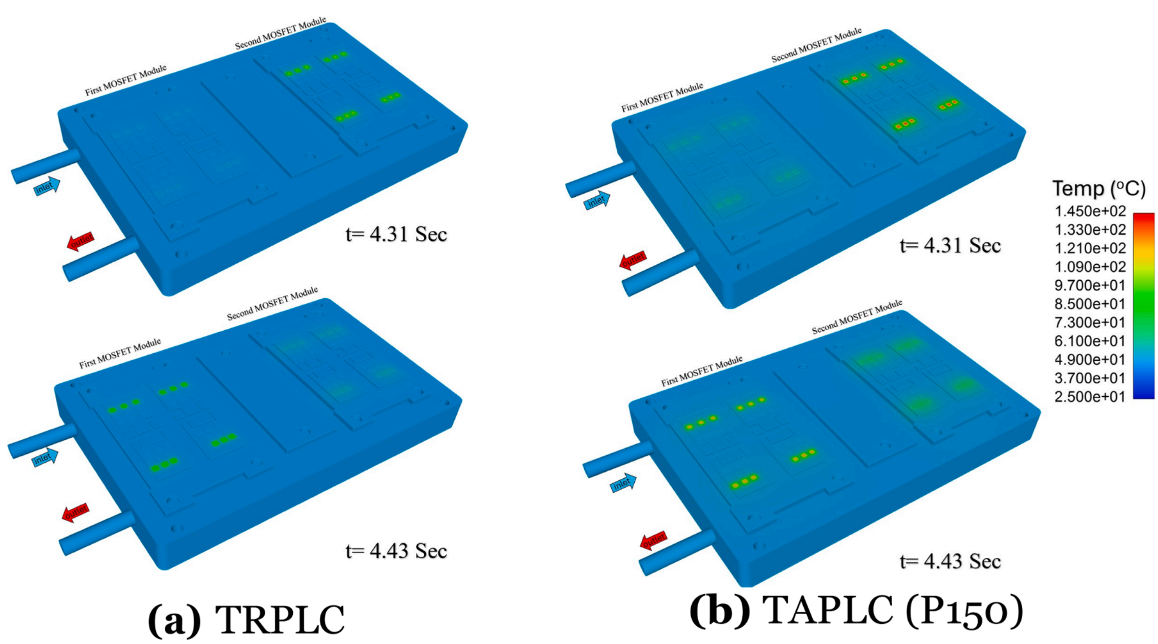

Fig. 8. Thermal mapping of converter's one leg.

module. By $t = 4.43$ s, the first MOSFET module becomes high while the second MOSFET module is low. As observed in the visuals, at $t = 4.43$ s, the second MOSFET module exhibits a slight decrease in temperature due to its low; however, it retains residual heat from the previous time step. If the second MOSFET module becomes high again in the subsequent time step, the power loss calculation will differ from the initial ($t = 0$ s) condition due to the retained temperature. As highlighted in this study, power loss is temperature-dependent, and the TRPLC approach captures this behav- ior accurately. When the TAPLC method is employed, assuming a high- temperature condition (P150) results in excessively elevated temperature, as seen in the visuals. Conversely, assuming a low-temperature condition (P25) yields unrealistically low temperatures. The results clearly demon- strate the significance of the TRPLC method, which dynamically considers the instantaneous temperature of the MOSFET to calculate power loss. This ensures that the outcomes closely resemble real-case scenarios, enhancing the accuracy and reliability of thermal simulations. By incorporating TRPLC, thermal management studies can achieve greater efficiency, minimizing unnecessary energy consumption for cooling. Additionally, optimized control algorithms based on accurate thermal data can improve system safety and extend the operational lifespan of MOSFET modules.

4. Conclusion

It is evident that Temperature-Agnostic Power Loss Calculation (TAPLC) methods used in the thermal simulations of power electronic com- ponents are insufficient for accurately estimating temperature distribution. This is primarily because the switching operations by semiconductor mate- rials enable the rapid passage and interruption of high amounts of energy in a very short time. This rapid energy transfer in semiconductor materi- als results in significant losses and heat generation, which directly affect the thermal properties of the material. Even though MOSFET manufacturers provide some information, the heat transfer characteristics within the MOSFET are influenced by numerous factors, including design, environment, cold plate, heat sink, and cooling fluid. Therefore, the information provided by MOSFET manufacturers alone is inadequate for a comprehensive analysis.

In this study, power loss graphs for the MOSFET module were plotted separately for junction temperatures of 25 °C, 100 °C, 125 °C, and 150 °C, and these graphs were converted into equations using the curve fitting method. The equations provide specific power loss data for each junction temperature as a function of the drain-source current. The key aspect of this study is that the power loss was recalculated at each time step based on the junction temperature, allowing the temperature profile, which changes over time, to directly impact the power losses. Furthermore, the design was analyzed in 3D, considering parameters such as cold plate, coolant velocity, coolant temperature, and ambient temperature. The results demonstrate that the junction temperatures obtained from TRPLC differ significantly from those calculated with a TAPLC assumption. This approach creates a study that closely resembles real experimental conditions, as opposed to the unidirec- tional heat transfer calculations typically used in conventional methods.

CRediT authorship contribution statement

Mustafa Ozden: Writing – review & editing, Writing – original draft, Visualization, Validation, Software, Methodology, Investigation. **Gokhan Ozkan:** Supervision. **S M Imrat Rahman:** Visualization, Methodology, Investigation. **Elutunji Buraimoh:** Writing – original draft. **Laxman Timilsina:** Investigation. **Behnaz Papari:** Software, Investigation. **Christopher S. Edrington:** Supervision.

Declaration of competing interest

The authors declare that they have no known competing financial interests or personal relationships that could have appeared to influence the work reported in this paper.

Acknowledgments

This work was supported by Clemson University's Virtual Prototyping of Autonomy Enabled Ground Systems (VIPR-GS) under Cooperative Agree- ment W56HZV-21–2–0001 with the US Army DEVCOM Ground Vehicle Systems Center (GVSC). DISTRIBUTION STATEMENT A. Approved for pub- lic release; distribution is unlimited. OPSEC9415. The authors would like to acknowledge the Warren H. Owen Distinguished Professorship Endowment for its support of the research effort.

Data availability

The authors do not have permission to share data.

References

[1] Y. Xu, C.N.M. Ho, A. Ghosh, D. Muthumuni, Design, implemen- tation, and validation of electro-thermal simulation for SiC MOSFETs in power electronic systems, IEEE Trans. Ind. Appl.- tions 57 (3) (2021) 2714–2725.

[2] L. Timilsina, P.R. Badr, P.H. Hoang, G. Ozkan, B. Papari, C.S. Edrington, Battery degradation in electric and hybrid electric vehicles: a survey study, IEEE Access 11 (2023) 42431–42462.

[3] L. Timilsina, P.H. Hoang, A. Arsalan, B.R. Badr, G. Ozkan, B. Papari, C.S. Edrington, Degradation abatement in hybrid electric vehicles using data-driven technique, Transp. Res. Procedia 70 (2023) 52–60.

[4] J. Wang, W. Chen, Y. Wu, J. Zhang, L. Wang, J. Liu, Chip-level electrothermal stress calculation method of high-power IGBT modules in system-level simulation, IEEE Trans. Power Electron. 37 (9) (2022) 10546–10561.

[5] G. Ozkan, P.H. Hoang, P.R. Badr, C.S. Edrington, B. Papari, Real-time thermal management for two-level active rectifier with finite control set model predictive control, Int. J. Electr. Power Energy Syst. 131 (2021) 107057.

[6] L. Xu, Y. Liu, S. Liu, Modeling and simulation of power elec- tronic modules with microchannel coolers for thermo-mechanical per- formance, Microelectron. Reliab. 54 (12) (2014) 2824–2835.

[7] W. Li, N. Mao, T. He, J. Gong, CFD Simulation of Novel adap- tive pin-Fins Microchannel Heat Sink to Improve Thermal Management of Electronic Chips, Applied Thermal Engineering, 2024 123667.

[8] S.M.I. Rahman, A. Moghassemi, A. Arsalan, L. Timilsina, P.K. Chamarthi, B. Papari, G. Ozkan, C.S. Edrington, Emerging Trends and Challenges in Thermal Management of Power Electronic converters: A state of the Art Review, IEEE Access, 2024.

[9] G. Ozkan, "Active Thermal Management and Fault-Tolerant Control For Switching Power Converters With Sequence-Based Control," Ph.D. disser- tation, The Florida State University, 2019.

[10] D. Karimi, H. Behi, J. Jaguemont, M. El Baghdadi, J. Van Mierlo, and O. Hegazy, "Thermal concept design of MOSFET power modules in inverter subsystems for electric vehicles," in *Proc. 9th Int. Conf. Power Energy Syst. (ICPES)*, 2019, pp. 1–6.

[11] Z. Shuai, S. He, Y. Xue, Y. Zheng, J. Gai, Y. Li, G. Li, J. Li, Junction temperature estimation of a SiC MOSFET module for 800V high-voltage application in electric vehicles, Etransportation 16 (2023) 100241.

[12] M. Shahjalal, T. Shams, S.B. Hossain, M.R. Ahmed, M. Ahsan, J. Haider, R. Goswami, S.B. Alam, A. Iqbal, Thermal analysis of Si-IGBT based power electronic modules in 50kW traction inverter ap- plication, e-Prime-Adv. Electr. Eng. Electron. Energy 3 (2023) 100112.

[13] A. Moghassemi, S.M.I. Rahman, G. Ozkan, C.S. Edrington, Z. Zhang, P. K. Chamarthi, Power Converters coolant: past, present, future, and a Path Toward Active Thermal Control in Electrified Ship Power sys- tems, IEEE Access, 2023.

[14] S. Hassan, P. Rajaguru, S. Stoyanov, C. Bailey, T. Tilford, Coupled thermal-mechanical analysis of power electronic modules with finite el- ement method and parametric model order reduction, Power Electron. Devices Compon. 8 (2024) 100063.

[15] B. Ramos-Alvarado, P. Li, H. Liu, A. Hernandez-Guerrero, CFD study of liquid-cooled heat sinks with microchannel flow field configu- rations for electronics, fuel cells, and concentrated solar cells, Appl Therm Eng 31 (14–15) (2011) 2494–2507.

[16] J. Rodriguez, S. Bernet, P.K. Steimer, I.E. Lizama, A survey on neutral-point-clamped inverters, IEEE Trans. Ind. Electron. 57 (7) (2009) 2219–2230.

[17] Z. Ma, H. Niu, X. Zhang, X. Wu, X. Cai, Virtual Space Vec- tor Over-Modul. Strategy NPC Three-Lev. Invert. Common-Mode Volt. Suppr. (2024).

[18] Z. Zhang, A. Anthon, M.A.E. Andersen, Comprehensive loss eval- uation of neutral-point-clamped (NPC) and T-Type three-level inverters based on a circuit level decoupling modulation, in: Proceedings of the 2014 International Power Electronics and Application Conference and Exposition, 2014, pp. 82–87.

[19] S.M.I. Rahman, G. Ozkan, A. Arsalan, P.K. Chamarthi, B. Papari, and C.S. Edrington, "Impact of active cooling on the thermal management of 3-level NPC converter for hybrid electric vehicle application," SAE Tech. Pap., no. 2023-01-1684, 2023.

[20] H. Liu, B. Li, R. Wang, MATLAB/FLUENT Co-optimization Framework for power budget allocation of mobile devices, in: Proc. 26th Int. Workshop Thermal Investigations of ICs and Systems, THER- MINIC, 2020, pp. 1–5.

[21] X. Dong, A. Griffo, D. Hewitt, J. Wang, Reduced-order thermal observer for power modules temperature estimation, IEEE Transac- tions Ind. Electron. 67 (12) (2019) 10085–10094.

[22] Wolfspeed, "BM2 62mm Power Module Family - CAS120M12BM2," Available: https://www.wolfspeed.com/bm2-62mm-power-module-family/cas120m12bm2. Accessed: 01-Jul-2024.

[23] X. Yang, K. Heng, X. Dai, X. Wu, G. Liu, A temperature- dependent Cauer model simulation of IGBT module with analytical thermal impedance characterization, IEEE J Emerg Sel Top Power Electron 10 (3) (2021) 3055–3065.

[24] R. Wu, F. Iannuzzo, H. Wang, F. Blaabjerg, An Icepak-PSpice co-simulation method to study the impact of bond wires fatigue on the current and temperature distribution of IGBT modules under short- circuit, in: Proc. IEEE Energy Conversion Congress and Exposition (ECCE), 2014, pp. 5502–5509.

[25] Y. Wang, X. Rong, C. Yang, H. Shi, J. Zheng, Multi-physics cou- pling analysis of high-power IGBT module bonding wires fault consid- ering stray inductance of main circuit, Microelectron. Reliab. 149 (2023) 115200.

Mustafa Ozden received his B.*Sc*. degree in Energy system engineering department, his M.*Sc*. and Ph.D. degrees in renewable energy systems from Erciyes University in 2015, 2017 and 2022, respectively. He was a postdoctoral researcher at Erciyes University from 2022 to 2023. He is presently working in the Energy Innovation Center at Clemson University as a postdoctoral fellow. He is a member of the Real-Time Control and Optimization Laboratory (RT-COOL). His current research interests include wind turbines, aerodynamic and thermo-mechanical modeling, and cooling system analysis.

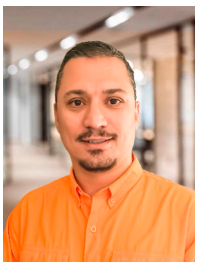

Gokhan Ozkan received the B.S. degree in teacher training from Marmara University, Turkey, in 2006, the B.S. degree in electrical field and energy system engineering and the M.S. degree in energy system engineering from Erciyes University, Turkey, in 2014 and 2016, respectively, and the Ph.D. degree in electrical and computer engineering from the FAMU-FSU College of Engineering. He was a Lecturer at Bozok University, Turkey. He worked as a Graduate Research Assistant with the Center for Advanced Power Systems, Florida State University. He is currently a Research Assistant Professor with the Real-Time COntrol and Optimization Laboratory (RT-COOL), Clemson University. His research interests include renewable energy real-time modeling, simulation, control design, and electro-thermal management for power converters.

S M Imrat Rahman received the B.*Sc*. degree in electrical and electronic engineering from the Islamic University of Technology, Bangladesh, in 2010, and the M.*Sc*. degree in power engineering from the Technical University of Munich, Germany, in 2015. He is currently pursuing the Ph.D. degree with the Holcombe Department of Electrical and Computer Engineering (ECE), Clemson University, under the supervision of Dr. Christopher S. Edrington and Dr. Gokhan Ozkan. He is a Graduate Research Assistant with the Real-Time COntrol and Optimization Laboratory (RT-COOL), Holcombe Department of ECE, Clemson University. His research interests include active thermal management of power electronic converters, distributed control, and thermal modeling of power electronic building blocks (PEBB) systems.

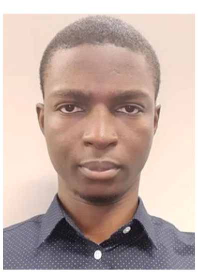

Elutunji Buraimoh received the Bachelor of Technology (B. Tech.) degree (Hons.) in electronic and electrical engineering from the Ladoke Akintola University of Technology, Nigeria, in 2012, the Master of Science (M.*Sc*.) degree in electronic and electrical engineering from Obafemi Awolowo University, Nigeria, in 2016, and the Doctor of Engineering (Ph.D.) degree in electrical engineering from the Durban University of Technology, South Africa. His research interests include inverter-based microgrids, renewable energy, power systems control, and FACTS devices.

Laxman Timilsina received the B.E. degree in electrical engineering from the Institute of Engineering, Tribhuvan University, Nepal, in 2016, the M.*Sc*. degree in distributed generation in electrical engineering from the Institute of Engineering, in 2019, and the Ph.D. degree in electrical engineering from Clemson University, in May 2024, under the mentorship of Dr. Christopher S. Edrington. Transitioning to the next phase of his academic journey, he enrolled with Clemson University, in Fall 2021, to pursue the Ph.D. degree. Concurrently, he was a Graduate Research Assistant with the Real-Time COntrol and Optimization Laboratory (RT-COOL), The Holcombe Department of Electrical and Computer Engineering, Clemson University, where he is currently a Postdoctoral Researcher Fellow. His research interests include electrified vehicles, integration of renewable energy, ship power systems, and smartgrids.

Behnaz Papari received the Ph.D. degree in electrical engineering from Florida State University, USA, in 2018. She was an Assistant Professor in power electronics engineering and the Manager of the Duke Energy Smart Grid Laboratory. She was associated with the Energy Production and Infrastructure Center (EPIC), University of North Carolina at Charlotte. She is currently with the Department of Marine Engineering Technology, Texas A\&M University at Galveston. She has expertise in power systems with an emphasis on modeling, analysis, control, planning, and optimization. Her specialties are distributed controls and decision analysis under uncertainty, applications on energy system modeling, and stochastic optimization. Her research interests include renewable energy sources, power and energy management, control of stand-alone and utility-interactive energy systems, distributed control of smart grids, stochastic analysis, and real-time power distribution system simulation and hardware-in-the-loop instantiation.

Christopher S. Edrington received the B.S. degree in engineering from Arkansas State University in 1999 and the M.S. and Ph.D. degrees in electrical engineering from the Missouri University of Science and Technology in 2001 and 2004, respectively. He was a DoE GAANN Fellow, an NSF IGERT Fellow, and a Grainger Foundation Fellow with the Missouri University of Science and Technology. He is currently the Warren H. Owen Distinguished Professor of electrical and computer engineering at Clemson University. He is the Lead of the Real-Time COntrol and Optimization Laboratory (RTCOOL) as well as the Co-Director of the Smart Energy and Propulsion Focus Area in the new VIrtual PRototyping for Ground vehicle Systems (VIPR-GS) Center. He has published over 170 papers, including two IEEE prize awards and multiple conference paper awards. He has graduated 23 M.S. students and 16 pHD. students (with three in process). He has six patents (in real-time stability and complexity metrics). His research interests include modeling, simulation, and control of electromechanical drive systems, applied power electronics, distributed control, integration of renewable energy, storage, and pulse power loads.